ACS OMEGA

Open Access

http://pubs.acs.org/journal/acsodf

Article

Experimental Studies to Reduce Usage of Fossil Fuels and Improve Green Fuels by Adopting Hydrogen−Ammonia−Biodiesel as Trinary Fuel for RCCI Engine

Elumalai Ramachandran, Ravi Krishnaiah,* Elumalai Perumal Venkatesan, Sreenivasa Reddy Medapati, Rajagopalan Sabarish, Sher Afghan Khan, Mohammad Asif, and Emanoil Linul

Cite This: https://doi.org/10.1021/acsomega.3c06327

Read Online

ACCESS | Metrics & More | Article Recommendations

ABSTRACT: This study investigates the feasibility of hydrogen addition to achieve lower emissions and higher thermal efficiency in an ammonia−biodiesel-fueled reactivity-controlled compression ignition (RCCI) engine. A single-cylinder light-duty water-cooled compression ignition (CI) engine was adapted to run in RCCI combustion with port-injected ammonia and hydrogen as low reactive fuel (LRF) and direct-injected algal biodiesel as high reactive fuel (HRF). In our earlier study, the ammonia substitution ratio (ASR) was optimized as 40%. To optimize fuel and engine settings, hydrogen is added in quantities ranging from 5 to 20% by energy share. The combustion, performance, and emission characteristics were investigated for the trinary fuel operation. The result shows that the 20% hydrogen premixing with 40% ammonia−biodiesel RCCI operation increased the peak cylinder pressure (CP), peak heat release rate (HRR), and cumulative heat release rate (CHRR) by 15.12, 25.15, and 26.68%, respectively. Ignition delay (ID) and combustion duration (CD) were decreased by 15.53 and 11.24%, respectively. The combustion phasing angle was advanced by 4 °CA. The brake thermal efficiency (BTE) was improved by 15.49%, and brake specific energy consumption (BSEC) was reduced by 21.92%. While the nitrogen oxide (NOx) level was significantly increased by about 31.82%, the hydrocarbon (HC), carbon monoxide (CO), smoke, and exhaust gas temperature (EGT) were reduced by 24.53, 28.16, 25.82, and 17.47% as compared to the optimized ASR40% combustion.

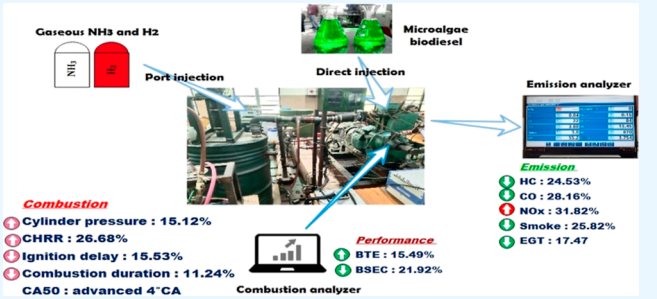

1. INTRODUCTION

The fast growth in carbon dioxide (CO_2) emissions over the centuries has raised the global temperature, which may have an influence on our humanity and create climatic problems. The most substantial greenhouse gas (GHG) is CO_2. Therefore, it could be necessary to restrict GHG emissions, particularly carbon emissions. The contemporary world depends on the efficient heat conversion technology of the internal combustion (IC) engine. About 70% of all carbon emissions are caused by the use of fossil fuels for energy, and IC engines constitute a significant contributor to this pathway of fossil fuel usage. However, the debate about the hazardous carbon and other emissions from IC engines fueled on petroleum-based fuels has centered on the production of renewable fuels. Controlling IC engine CO_2 emissions might thereby promote GHG reduction. Increasing the use of carbon-free energy sources is one way to reduce the carbon emissions from internal combustion engines because of their beneficial combustion characteristics and clean combustion products. Ammonia and hydrogen are the two different carbon-free energy sources that have recently attracted the most attention. Hydrogen and ammonia may be burned together without emitting carbon dioxide, and this combination performed well in both compression ignition (CI) and spark ignition engines. However, when compared to other types of automotive engines, CI provides superior fuel efficiency, less maintenance, and higher power.

1.1. Biodiesel as IC Engine Fuel. The main drawback of using ammonia and hydrogen in a CI engine is the high autoignition temperature. Therefore, these fuels are utilized with fuels with lower autoignition temperatures. However, the use of fossil fuels, such as diesel, would result in increased fuel consumption and a range of environmental pollutants. In CI engines, biodiesel is being considered as an alternative sustainable fuel to fossil fuels. This enables CI engines to run entirely on renewable fuel while emitting minimal pollution and a higher performance. Biodiesel is an alternative

Received: August 31, 2023
Revised: October 18, 2023
Accepted: October 20, 2023

fuel used by diesel engines as it is easily accessible, environmentally friendly, nontoxic, renewable, and has a low sulfur concentration. Kukana and Jakhar[1] experimented with the impacts of biodiesel on CI engines. The result revealed that the use of biodiesel exhibits a maximum heat release rate (HRR) and peak cylinder pressure (CP). Break thermal efficiency (BTE) and brake specific energy consumption (BSEC) are higher than those of conventional diesel, while nitrogen oxide (NOx) emissions and other pollutants are reduced. Shrivastava et al.[2] investigated the influence of biodiesel on emissions and performance properties in diesel engines. The investigation results reveal that the BTE of biodiesel is 4.87% higher than that of conventional diesel. Tizvir et al.[3] studied the effect of biodiesel. The findings showed that using 10 and 20% biodiesel, respectively, decreased carbon monoxide (CO), hydrocarbon (HC), and NOx emissions by 9.2, 7.3, and 2.9, and 23.5, 18.3, and 6.9%, respectively. For B10 and B20, respectively, CO_2 output rose by 1.3 and 5.4%. The use of biodiesel instead of diesel has reduced pollutants. Ogunkunle and Ahmed[4] studied the impact of biodiesel in a CI engine. The results revealed that biodiesel increased NOx emissions while reducing CO and CO_2 emissions by 81.7 and 65.7%, respectively. Raman et al.[5] investigated the diesel engine characteristics utilizing rapeseed biodiesel and came to the conclusion that biodiesel enhances the engine's performance with high thermal efficiency and low exhaust emissions.

1.2. Ammonia as IC Engine Fuel. According to a study, ammonia or an ammonia and hydrogen blend would be the primary fuel for IC engines that would achieve the 2050 renewable energy goal.[6] Ammonia has several benefits as a substitute fuel, including its absence of a carbon structure, lowest storage cost, simplicity of production, improved calorific value, and energy conservation. The combustion of ammonia produces no carbon emissions, which meets international regulations. A further benefit is that ammonia is in its liquid phase at 273 K and around 8 atm, which makes it easier to store and transport. The autoignition temperature of ammonia is greater than the autoignition temperature of hydrogen and hydrocarbon fuels, and ammonia fuel has a much lower propensity to explode if inadvertently leaked during usage or storage. Also, quick action can be taken to avoid an accident by smelling ammonia in the case of leakage. Ammonia's potential as a renewable fuel for CI engines is considered because of its excellent properties. Ammonia's high-octane level provides a decreased propensity to knock, making it the ideal supplemental fuel for high-compression-ratio CI engines. In an effort to enhance combustion, performance, and emission, a diesel pilot injection approach was adopted, with the direct injection energy ratio ranging from 0 to 100%. To further confirm the viability of the diesel direct injection, ammonia energy proportions of 40 to 70% were used for this technique. According to the results, the direct injection technique could lower NH_3 emissions. N_2O emissions were also reduced. A greater thermal efficiency of around 45% may also be maintained using the pilot-injection technique. Low CO_2 emissions and steady combustion were obtained. However, the pilot-injection approach has drawbacks due to greater NOx, HC, and CO emissions.[7] The impact of split injection in a diesel−ammonia mixture on the CI engine is examined. According to the result, when related to diesel combustion, there was a 4−7% enhancement in the thermal efficiency. HC emissions decreased by 50−67%, smoke emissions rose by 8−13%, NOx emissions increased by 7−19%, and CO_2 emissions increased by 2−10%.[8] The viability of ammonia energy was investigated by using a diesel−ammonia dual-fuel CI engine. The findings demonstrate that diesel injection might lower ammonia emissions while maintaining a high thermal efficiency of around 45%. Low CO_2 emissions and steady combustion were attained by the engine at a greater ammonia energy premixed ratio. However, increased emissions of HC, CO, and NOx were noted.[7] The ammonia dual-fuel engine was developed to examine the feasibility of utilizing ammonia in a four-stroke CI engine. The usage of ammonia raised N_2O emissions by 0.18 to 0.49 g/kW h, which corresponds to 0.06 to 0.1% nitrogen in ammonia fuel, partly offsetting the reduction in CO_2 emissions, according to the results.[9] A variable compression ratio in an ammonia combustion technique is used in an experimental investigation. According to the findings, raising the compression ratio improved thermal efficiency and NOx.[10]

1.3. Hydrogen as IC Engine Fuel. The utilization of energy-efficient hydrogen combined with the use of different fuels is the main focus of research on ignition engines for road and bridge transmissions. Fuel efficiency is expected to be significantly improved by hydrogen enrichment. Hydrogen can be produced from a variety of sources, such as biomass, nuclear energy, the sun, and wind. The inclusion of hydrogen as an energy carrier improves the performance of the base fuel. As a single, clean source of energy, hydrogen may also be used to improve the performance of alternative fuels. The physiochemical properties of hydrogen set it apart from those of other fuels. The direct use of hydrogen fuel in diesel engines has some drawbacks. Instead, using hydrogen as a dual fuel with low autoignition fuel seems more feasible. In dual-fuel engines, many researchers are looking at alternative fuels to diminish pollution and increase energy efficiency. The most notable of these fuels is hydrogen. Köse and Ciniviz[11] examined the impact of hydrogen energy in an investigation and found a tendency of increasing BTE with reduced BSEC and reduced exhaust engine-out emissions. Qin et al.[12] examined the diesel engine's performance using various hydrogen ratios. They discovered that using a 20% hydrogen ratio resulted in a 7.7% increase in the maximum cylinder pressure (CP). The same research also revealed that HRR increased and became apparent early in the process. In an investigation, the effect of hydrogen on combustion efficiency and emissions was investigated. Results revealed that, when the hydrogen energy proportion was 7%, a 40% reduction in soot emissions was observed, 33% of CO emissions were decreased, and the thermal efficiency was improved as compared to pure diesel.[13] In an investigational study, the effects of the hydrogen energy proportion on efficiency and emissions were investigated. From the experimental findings, the thermal efficiency was enhanced by 18.4% for the hydrogen-enriched fuel. BSEC decreased by 13.6%. Although NOx emissions increased significantly, HC, CO, and smoke were reduced. In research, the effect of the hydrogen energy ratio on dual-fuel CI engines at various hydrogen flow rates was examined. Increases in hydrogen flow rate result in a 52.04% rise in the CP. The engine torque has increased by 95.53%, and the HRR from the burning of the hydrogen charge is more intense.[14] Thermal efficiency increased by 25%, while BSEC decreased by 92.27% for the designated hydrogen flow rate. Additionally, CO emissions decreased, whereas CO_2 and NOx emissions continued to increase.[15]

https://doi.org/10.1021/acsomega.3c06327
ACS Omega XXXX, XXX, XXX−XXX

1.4. Reactivity-Controlled Compression Ignition. To address the complexity of stringent emission laws, many scientists examined the potential of low-temperature combustion (LTC). The concept of LTC has attracted significant interest worldwide as it can simultaneously reduce NOx and PM emissions in IC engines. Also, the dual-fuel combustion concept is one of the most promising LTC concept achieving strategies. To enhance efficiency and reduce the NOx/soot trade-off in CI engines, reactivity-controlled compression ignition (RCCI) is taking into consideration one of the various LTC strategies. It is used with two distinct types of fuel, notably PFIs (port fuel injections) with low reactive fuel (LRF) and DI (direct injection) with high reactive fuel (HRF). When the circumstances are favorable, autoignition occurs. The major portion of energy is generated primarily by port fuel; a significant quantity of the LRF fuel is homogeneously mixed and has a key impact in obtaining high efficiency with significant reductions in NOx pollutants. Curran et al.[16] investigated the impact of RCCI operation on a CI engine. The thermal efficiency of RCCI increased by 7%; NOx emissions decreased, whereas HC and CO emissions increased in comparison to diesel operation. An increase in BTE and lower BSEC are understood as a result of lower heat losses. An investigation was conducted to investigate the combustion of RCCI. According to research findings, the amount of RCCI burned at full load increased BTE, maximal CP, and net HRR by 0.2−1.2, 4.9−13.6, and 11.3−44.6%, respectively. Similar to this, at maximum loads, the RCCI method dramatically lowers NOx and soot emissions by 24.4−43.7 and 31.3−52.6%, respectively. However, compared to conventional biodiesel, CO and HC emissions are greater.[17] An investigation was carried out on RCCI combustion by evaluating the emission performance of a CI engine, it was discovered that the homogeneity of the air fuel mixture largely controls the NOx emissions of RCCI. Additionally, raising the premixed ratio may successfully enhance BTE and NOx while reducing the peak pressure rise rate for RCCI.[18]

1.5. Motivation and Objective. The principal goal of the inquiry is to maximize the utilization of carbon-free and carbon-neutral renewable fuels. Since ammonia has certain inadequacies in combustion attributes for compatibility, suggesting it as a substitute for petroleum-based fuels on engine-out attributes is deficient. Ammonia has the lowest adiabatic flame temperature, lower laminar flame speed, and higher latent heat of evaporation, which leads to decreased thermal efficiency. Conversely, the use of hydrogen in diesel engines provides a significant effect on engine-out attributes. Consequently, hydrogen behavior studies are needed to minimize ammonia combustion defects due to hydrogen's superior properties. Therefore, a comprehensive investigation was conducted to analyze the effect of ammonia on hydrogen on diesel engines by using biodiesel as an ignitor. Nevertheless, the majority of the study focuses on ammonia energy sharing with conventional fuels, such as biodiesel, diethyl ether, and so on. However, the goal of the initiative is to improve the combustion of carbon-free fuels in CI engines, while lowering the need for biodiesel. Therefore, a complete investigation of the RCCI behavior with trinary fuels on combustion, performance, and emission properties under all load conditions is required to reach high-quality ammonia combustion in diesel engines. Because of the better characteristics of hydrogen, enriching it with ammonia enhances combustion efficiency. However, hydrogen induction to 40% ammonia premixing is limited to 20% hydrogen because the induction of ammonia and hydrogen replaces the essential air required for combustion.

According to the literature, the combustion characteristics of ammonia have been investigated in combination with other fuels. However, ammonia, biodiesel, and hydrogen-powered RCCI engine combustion have not been dealt with in depth. The research suggests accelerating the combustion of ammonia using hydrogen as an additive fuel for RCCI combustion. The aim of the current investigation is to focus on how different hydrogen energy proportions are combusted into the ammonia−biodiesel mixture as ternary fuels in a dual-fuel engine. This type of study may support an increase in the usage of carbon-free fuels in CI engines.

2. EXPERIMENTAL METHODOLOGY

2.1. Energy Fraction Methodology. The energy fractions of hydrogen and ammonia are calculated by eq 1 and are described as the energy proportion of ammonia and hydrogen to the total supplied energy. Where m_A, m_H, and m_B are the mass flow rates of ammonia, hydrogen, and biodiesel discretely, CV_A, CV_H, and CV_B are the heating capacities of hydrogen, ammonia, and biodiesel

$$\text{Energy share (\%)} = \frac{(m_A \times CV_A) \text{ or } (m_H \times CV_H)}{(m_B \times CV_B) + (m_A \times CV_A) + (m_H \times CV_H)} \times 100 \quad (1)$$

Before starting the data acquisition process, the investigation engine is warmed to 80 °C to provide stable operating conditions. To control the degree of error in the collected data, the experiments were conducted three times, and estimates were completed by averaging the findings. Tables 1 and 2 show the properties and flow rates of various fuels.

Table 1. Test Fuel Properties

properties	ammonia	hydrogen	microalgae biodiesel
density (kg/L)@20°C	0.732	0.08	0.876
viscosity (mm^2/s)@40°C			5.07
octane number	130	130	
cetane number			42
calorific value (MJ/kg)	18.5	141.79	41.078
flame velocity (cm/s)	32	325	80
latent heat of vaporization (kJ/kg)	1372	461	306
mass diffusivity (cm^2/s)	0.23	0.62	
autoignition (°C)	652	585	250
fire point (°C)	148		121
flammability limit (% vol)	14−33.8	4−75	0.6−7.52
stoichiometric air/fuel	6.1	34.4	

2.2. LRF Supply System. The hydrogen gas is kept at 150 bar in a storage cylinder and is delivered into the inlet manifold through a regulator, mass flow meter, flame arrester, and flame trap. The induction of gaseous fuel begins at 355 °CA bTDC, and the induction valve for hydrogen remains open throughout. Similarly, a 150 bar ammonia storage cylinder is utilized to store the liquefied ammonia, and the bottom of the cylinder is heated at 39 °C by a heater that is fixed to the liquified ammonia storage cylinder and routed via a pressure regulator, a flow meter, and finally an injector. A gas chamber

https://doi.org/10.1021/acsomega.3c06327
ACS Omega XXXX, XXX, XXX−XXX

Table 2. Investigational Energy Matrix

energy fraction	mass flow rate ($\times 10^{-2}$ kg/h)														
	20% load				40% load			60% load			80% load			100% load	
acronym	A	H	BD	A	H	BD	A	H	BD	A	H	BD	A	H	BD
ASR40% + 0% H	34.1	0.0	22.6	54.6	0.0	36.3	66.3	0.0	44.0	75.9	0.0	50.4	88.9	0.0	59.0
ASR40% + 5% H	33.4	0.5	20.3	53.0	0.9	32.2	63.6	1.0	38.7	72.1	1.2	43.9	83.6	1.4	50.9
ASR40% + 10% H	32.8	1.1	18.1	51.4	1.7	28.4	61.1	2.0	33.8	68.5	2.2	37.9	78.6	2.6	43.5
ASR40% + 15% H	32.1	1.6	16.0	49.8	2.4	24.8	58.6	2.9	29.2	65.1	3.2	32.4	73.9	3.6	36.8
ASR40% + 20% H	31.5	2.1	13.9	48.3	3.2	21.4	56.3	3.7	24.9	61.8	4.0	27.4	69.4	4.5	30.7

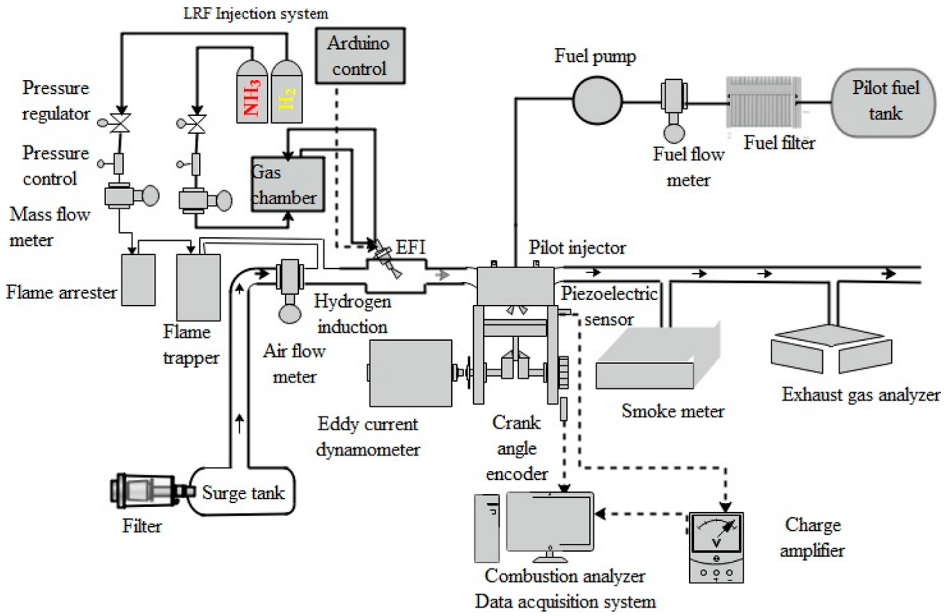

Figure 1. Experimental setup.

is introduced before the ammonia injectors to reduce the flow fluctuation triggered by pressure variations. Ammonia gas is fed into the cylinder through an electronically controlled solenoid port fuel injector. Pulse duration and injection timing were controlled by the electronic control unit (ECU). In both cases, a regulator controls the gas flow by reducing excessive inlet pressure to a suitable outlet pressure. The gaseous fuel mass flow rate is controlled by a precision flow control valve. The final hydrogen induction pressure is maintained at around 3.11 bar and the ammonia pressure before the injectors is maintained at around 4.81 bar. In the hydrogen induction circuit, a flashback arrestor is used to prevent backflow into the system. Finally, a flame trap was connected to direct the hydrogen, hence reducing the propensity for flash in the circuit.

2.3. Operating Condition. The properties of the CI engine powered by ammonia−hydrogen−biodiesel have been assessed in this study. The ammonia energy contribution in premixing is 40%, hydrogen enrichment ranges from 5 to 20%, and the remaining energy is microalgae biodiesel under various loads while keeping an identical engine speed of 1500. Ammonia requires a greater mass flow proportion to produce an identical quantity of power since it has less heat capacity than hydrogen and biodiesel. The charge stoichiometric ratio rises when hydrogen premixing increases because hydrogen has a greater stoichiometric ratio.[19] Further enrichment reduced the intake of oxygen. As a result, hydrogen enrichment is restricted to 20% in our present investigation. Table 2 shows the experimental matrix.

2.4. Investigational Engine Setup. The engine experimental setup for the investigation is presented in Figure 1. Tables 3 and 4 contain more details on the engine configuration, measurement uncertainty, and instrument precision. The noncontact speed sensor detects speed and the load cell measures load. An adjustable water-cooling system with a flow meter is provided to keep the dyno and engine at the proper temperature. K-type thermocouple sensors are

Table 3. Engine Particulars

parameters	details
made	Kirloskar
ignition	CI
no. of strokes	4
no. of valves	2
cooling method	water cooling
rated power (kW)	3.5
compression ratio	17.5
biodiesel injection	24°CA bTDC
speed (rpm)	1500
bore (mm)	87.5
stroke length (mm)	110
injection pressure (bar)	230
torque (N m)	23.5
dynamometer	eddy current

https://doi.org/10.1021/acsomega.3c06327
ACS Omega XXXX, XXX, XXX−XXX

Table 4. Uncertainty Examination[a]

variables	% accuracy	% uncertainty
Brake power (kW)	±0.5	±0.7
pressure (bar)	±0.41	±0.8
fuel consumption (g/s)	±0.62	±0.9
speed (rpm)	±0.26	±1.2
hydrocarbon (ppm)	±5.25	±0.8
carbon monoxide (% vol)	±0.08	±0.9
smoke opacity (%)	±1.33	±1.4
nitrogen oxides (ppm)	±2.35	±1.3

[a] The uncertainty in the experiment is $= \sqrt{0.8^2 + 0.7^2 + 0.9^2 + 1.2^2 + 0.8^2 + 0.9^2 + 1.4^2 + 1.3^2} = 2.91\%$.

precisely positioned at the required junctions to monitor the temperature. A Kistler piezoelectric pressure transducer is installed with a charge amplifier in the cylinder head to collect pressure data. For each operating condition, pressure data from 100 standard successive cycles was collected using an AVL crank angle encoder with an accuracy of 0.2 CAD. In order to observe the intake air and fuel consumption rates for performance studies, an anemometer and thermal mass flow meter (FOX, US make) are used. Pilot fuel is injected using a conventional fuel injection system and controlled by a mechanical governor. The air intake temperature, pressure, and exhaust back pressure were maintained at 38 °C, 1.34 bar, and 1.4 bar, respectively. The NI USA data acquisition system, which has a data collection rate of 250 kHz, is used to acquire data from all sensors. Utilizing the collected data, the engine software package calculates the performance variables. The AVL model 437 smoke opacity meter is utilized to quantify smoke emissions, while the AVL 444 Digas gas emission analyzer is utilized to assess HC, CO, and NOx emissions.

Kistler-made piezoelectric transducers and charge amplifiers are used in the data collection system to measure CP. The CP data was collected for 100 consecutive cycles to obtain a precise response rate for the study of combustion parameters. The governor effect controlled the pilot-injected biodiesel quantity, while the gaseous fuel quantity was manually adjusted. K-type thermocouple sensors are correctly installed at the corresponding junctures to track the temperature of cooling water, engine oil, input air, and exhaust gas. For collecting crank positioning data, a crank angle encoder sensor with 0.1 °CA resolution is installed at the end of the crankshaft.

2.5. Uncertainty. To ensure reproducibility of experimental findings within measured uncertainties, observations were performed three times at each operational state, and the mean value is depicted in all figures. Table 4 shows the normal uncertainty in the observation of each of the essential parameters with 95% assurance (i.e., $+2\sigma$ limits).

The uncertainty of the observed variable is specified as $(\Delta X_i) = 2\sigma_i / \overline{X}_i \times 100$.

For the derived variables, the quadratic mean method is utilized to offer precise uncertainty limits, and eq 2 expresses the level of precision

$$\Delta R = \sqrt{\left(\frac{\partial R}{\partial x_1} \times \Delta x_1\right)^2 + \left(\frac{\partial R}{\partial x_2} \times \Delta x_1\right)^2 + \cdots \left(\frac{\partial R}{\partial x_n} \times \Delta x_n\right)^2} \quad (2)$$

3. RESULTS AND DISCUSSION

3.1. Combustion Factors. *3.1.1. Cylinder Pressure.* The relation between CP and crank angle is essential for determining quantitative data about combustion. In the process of hydrogen addition to ASR40% combustion, the peak CP is advanced because the flame velocity increases when hydrogen is added to the combustion because hydrogen has higher reactivity.[20] Figure 2 depicts the CP values for various

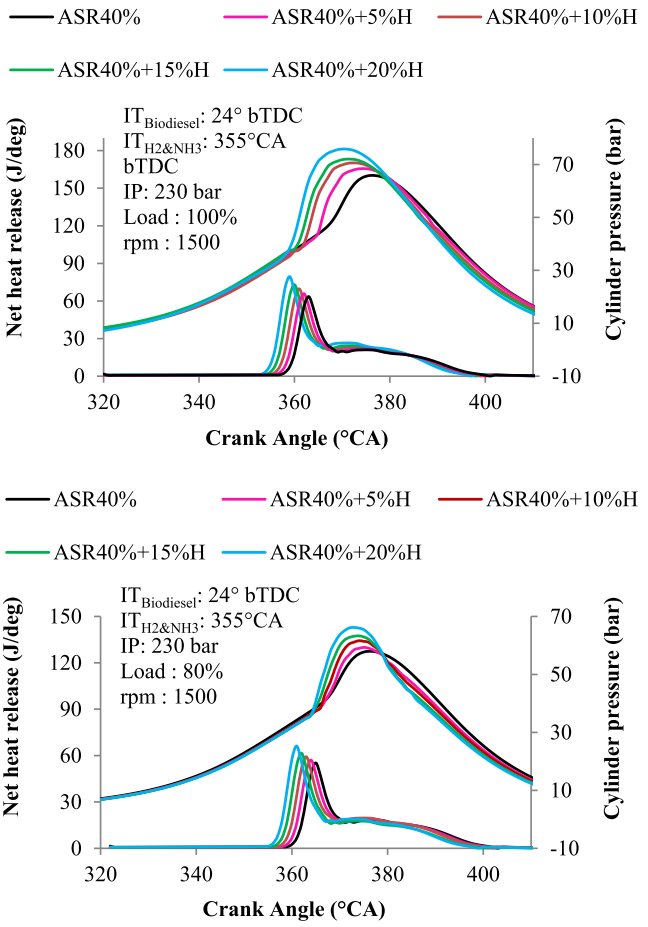

Figure 2. In-cylinder pressure and heat release rate for various hydrogen enrichment processes.

test fuels. The peak CP values at maximum load are 65.9, 68.4, 70.6, 72, and 75.8 bar for ASR40%, ASR40% + 5% H, ASR40% + 10% H, ASR40% + 15% H, and ASR40% + 20% H operations, respectively. When compared to ASR40% combustion, the CP of the combustion chamber is increased by 3.9, 7.2, 9.4, and 15.1%, respectively. Ammonia and biodiesel combustion are enhanced when hydrogen is enriched, resulting in higher CP. With rising hydrogen energy, the duration of ID diminishes, and combustion advances progressively toward TDC, as illustrated in Figure 3. As a result, increasing the rate of hydrogen addition improves flame propagation, which leads to better combustion and reduces the ammonia escape phenomenon. Additionally, the biodiesel inbound oxygen succeeded in reducing the intake oxygen reduction. The highest CP is achieved with 20% hydrogen addition, and any further enrichment of hydrogen might trigger the engine to vandalize as the pressure rise rate exceeds engine design standards. When the load increases, the peak cylinder pressure and peak HRR also increase, and the occurrence of

https://doi.org/10.1021/acsomega.3c06327
ACS Omega XXXX, XXX, XXX−XXX

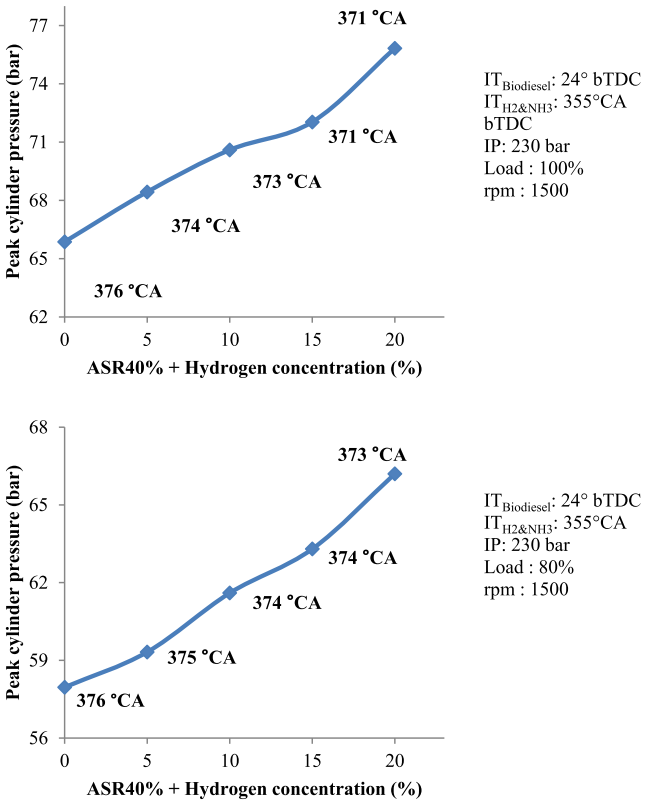

Figure 3. Peak cylinder pressure occurrences for different hydrogen enrichment processes.

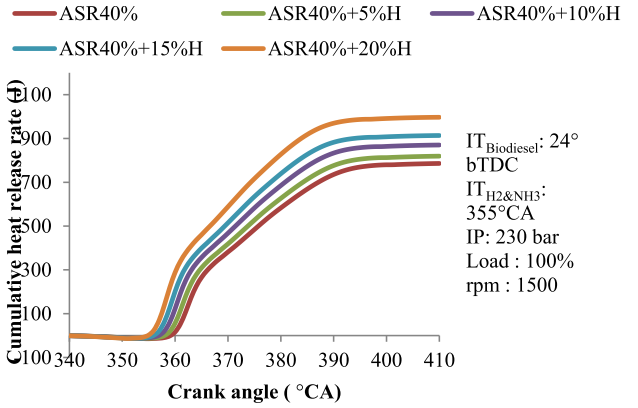

Figure 4. CHRR for different hydrogen enrichment processes.

the peak pressure and peak HRR increases due to the combustion temperature. This is illustrated in Figures 2 and 3.

3.1.2. Heat Release Rate. Instead of raising the fuel cetane number, one can enhance the combustion rate by fuel premixing. At maximum load, peak HRR of the engine was recorded as 63.51, 65.85, 69.71, 73.01, and 79.48 J/deg for ASR40%, ASR40% + 5% H, ASR40% + 10% H, ASR40% + 15% H, and ASR40% + 20% H operations, respectively. In comparison to the ASR40% process, the engine's peak HRR was improved by 3.69, 9.76, 14.95, and 25.15%. Figure 2 illustrates how the HRR fluctuates for various proportions of ASR40% operations. According to Pinto et al.,[21] the combustion process of the dual fueling concept is clearly explained into three steps: pilot fuel combustion, premixed port fuel combustion, and diffused pilot/port fuel-controlled combustion. In this manner, the HRR related to the port fuel is increased, which quickens the mixture combustion and enhances the intensity of the initial phase of HRR. Additionally, due to the reduced ID of the hydrogen-enriched ammonia−biodiesel combustion, which had an influence on greater HRR in the premix combustion phase, the fuels' HRR curves resemble those of the ammonia−biodiesel fuel. The higher heating value of hydrogen also contributes to higher HRRs. The increase in the gaseous hydrogen heating value and flame velocity, which produced progressive combustion in turn, was the main factor causing higher HRR for the hydrogen-enriched fuels. Therefore, hydrogen induction had a superior impact, such as extending the phase of premixed combustion instead of diffusion combustion because of its earlier SoC.[22] Hydrogen enrichment enhanced premixed combustion and peak HRR as compared to ASR40% dual fuel operation. The 20% hydrogen enrichment of ammonia−biodiesel has HRR curves greater than those of all other tested fuels. The enrichment of hydrogen in the combustion boosted the HRR, which, in turn, increased the fuel homogeneous combustion rates at higher flow rates of hydrogen. This outcome is consistent with those of earlier findings.[23] The commencement of combustion is indicated by the abrupt increase in HRR. Due to the increased fuel burning in the premixed combustion phase, the HRR unexpectedly rose, and peak HRR advanced for the hydrogen enrichment combustion.

3.1.3. Cumulative Heat Release Rate. The cumulative heat release rate (CHRR) for different hydrogen-enriched combustions is illustrated in Figure 4. CHRR is an important parameter to characterize the efficiency of the combustion process. At maximum load, the recorded CHRR was 779.02, 811.85, 861.97, 904.67, and 986.91 J for ASR40%, ASR40% + 5% H, ASR40% + 10% H, ASR40% + 15% H, and ASR40% + 20% H operations, respectively. In comparison to ASR40% combustion, the observed CHRR is enhanced by 4.21, 10.65, 16.13, and 26.68%. As can be noted, hydrogen enrichment combustion had an earlier SoC and a shorter late combustion. This is due to the fact that the superior characteristics of hydrogen burn the ammonia that has already been inducted. An increase in hydrogen proportion, earlier SoC, and shorter late combustion was observed as results. This is because the enhanced combustion response and shorter ID allow for an earlier autoignition time of ammonia owing to the hydrogen adiabatic flame temperature. As hydrogen concentration increased, the duration of combustion steadily decreased because higher mass diffusivity of hydrogen leads to enhanced combustion of ammonia and biodiesel, which led to greater CHRR and higher flame velocity of hydrogen, which led to an accelerated combustion process.[24] The CHRR also grew by about 26.68% when 20% hydrogen enrichment was used for 40% ammonia energy shared with biodiesel.

3.1.4. Ignition Delay. Co-firing ammonia with hydrogen and highly reactive fuel is an effective method to decrease ammonia's resistance to autoignition and get around problems with employing NH_3 in diverse applications has been suggested. For ammonia applications, it is crucial to investigate the ID time of NH_3, which also aids in the interpretation of the oxidation chemistry of NH_3 at low temperatures. At maximum load, the recorded ID period was 15.52, 14.45, 13.95, 13.48, and 13.11 °CA for ASR40%, ASR40% + 5% H, ASR40% + 10% H, ASR40% + 15% H, and ASR40% + 20% H operations, respectively. In comparison to ASR40% combustion, the

https://doi.org/10.1021/acsomega.3c06327
ACS Omega XXXX, XXX, XXX−XXX

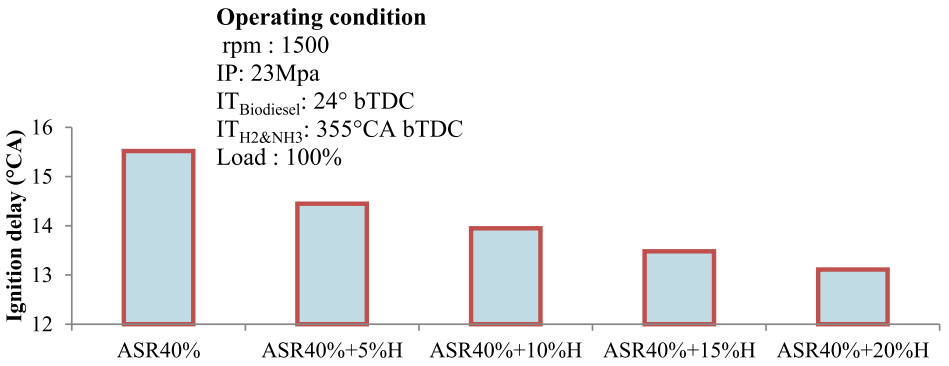

Figure 5. Ignition delay for different hydrogen enrichment processes.

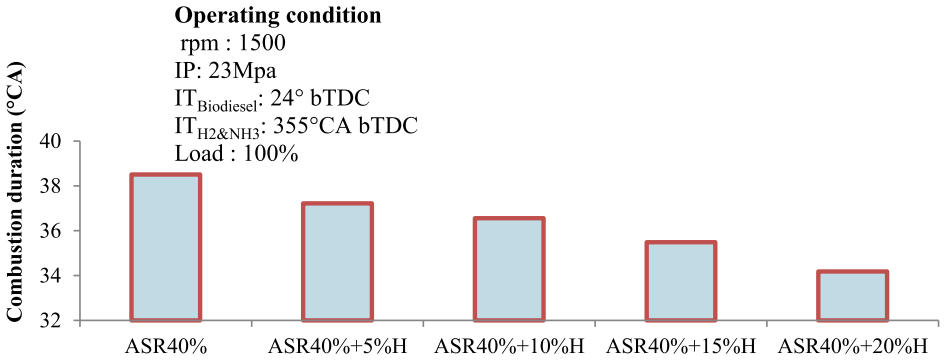

Figure 6. Combustion duration for different hydrogen enrichment processes.

engine's ID period decreased by 6.89, 10.11, 13.15, and 15.53%. Due to the slower flame speed and lower adiabatic flame temperature of ammonia, the burning duration was longer, and a lower peak combustion temperature was recorded. The flame initiation duration and CD were increased for the ASR40% combustion operation. The slow laminar flame speed, the lowest adiabatic flame temperature of NH_3, and the necessity for elevated ignition energy cause a delay in the growth of the flame-kernel that affects the flame initiation and CD. It is clear from Figure 5 that the enrichment of H_2 significantly increases the ammonia reactivity by lowering the ID. Hence, a 20% H_2 addition enhanced the NH_3 reactivity at LTC circumstances and shortened ID than the other tested fuels. According to the findings, the measured ID times for hydrogen-enriched ammonia−biodiesel reveal that they are suitable for LTC engines.

3.1.5. Combustion Duration. It is clear that burning ammonia and biodiesel together causes the CD to be longer and the combustion temperature to be much lower. Under the current operating manner, the greater ammonia emissions might possibly be attributed to the reduced combustion temperature. At maximum load, the recorded CD period was 38.51, 37.22, 36.56, 35.49, and 34.18 °CA for ASR40%, ASR40% + 5% H, ASR40% + 10% H, ASR40% + 15% H, and ASR40% + 20% H operations, respectively. In comparison to ASR40% combustion, the engine's CD period decreased by 3.35, 5.06, 7.84, and 11.24%. Ammonia's slower flame speed makes the combustion rate slower, necessitating extended CD. As a result of the ammonia late combustion, the expansion pressure is a little bit greater in the dual-fuel situation. Additionally, since gaseous fuels are introduced during the suction stroke, there is enough time to produce a homogeneous gaseous charge within the cylinder before combustion begins. Therefore, the increase in premixed charge quantity of hydrogen with ammonia inside the engine cylinder increased charge homogeneity, resulting in better premixed combustion phase characteristics, which correspondingly reduced the CD.

Another reason could be that more heat is generated during the premixed combustion phase with ammonia−hydrogen fueled RCCI, which reduces the CD of the hydrogen-enriched test fuel. Figure 6 demonstrates that, as contrasted to the ASR40% fueled RCCI mode, combustion time reduced as the hydrogen energy share increased. It went from 38.51 °CA with the basic ammonia−biodiesel dual fuel mode to 34.18 °CA with a 20% H_2 energy share. The molar proportions of OH and O radicals rise with the enrichment of hydrogen to ammonia, improving the reactivity of the ammonia charge and resulting in reduced combustion duration and a higher percentage of constant-volume combustion.[25,26] Therefore, the settings may result in an increase in the engine's BTE.

3.1.6. Combustion Phasing Angle. The term "CA50" refers to the crank angle at which 50% of the fuel burns. The combustion center is one of the key elements influencing engine performance and emissions. There is a linear link between the hydrogen addition and CA50. When the hydrogen energy increases, CA50 shifts to TDC. Figure 7 demonstrates how combustion progresses when hydrogen energy rises. The combustion phase angle shifts toward TDC and CHRR at CA50, increasing as the hydrogen premixing rises with the optimal 40% ammonia−biodiesel RCCI operation since the combustion of the NH_3−biodiesel mixture is increased by hydrogen adiabatic flame temperature and flame speed.[27,28] When using hydrogen enrichment for ammonia−biodiesel, CA50 was advanced to 4 °CA, which resulted in the advancement of the combustion center. Investigations are

https://doi.org/10.1021/acsomega.3c06327
ACS Omega XXXX, XXX, XXX−XXX

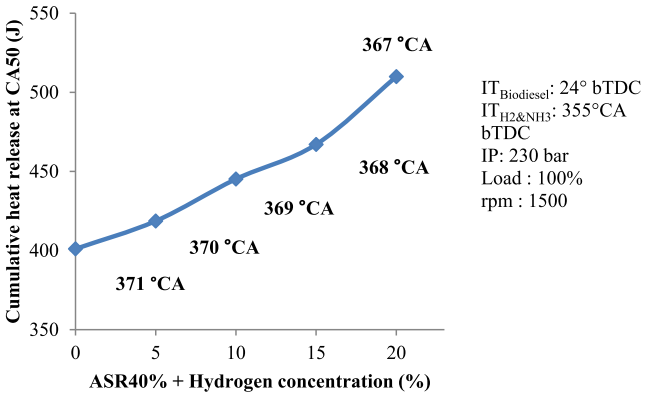

Figure 7. Combustion phasing angle for different hydrogen enrichment processes.

limited since the highest thermal efficiency is achieved when the combustion center is located at 7 °CA aTDC for 20% H_2 enrichment with ammonia biodiesel operation. It was reported that a similar trend of maximum thermal efficiency was obtained at CA50 for 5 to 11 °CA aTDC.[29,30]

3.2. Performance Factors. *3.2.1. Brake Thermal Efficiency.* BTE is the ratio of the brake shaft power output (power available in the crankshaft) to the rate of spent thermal energy of the fuel to generate that effort. Figure 8 elucidates

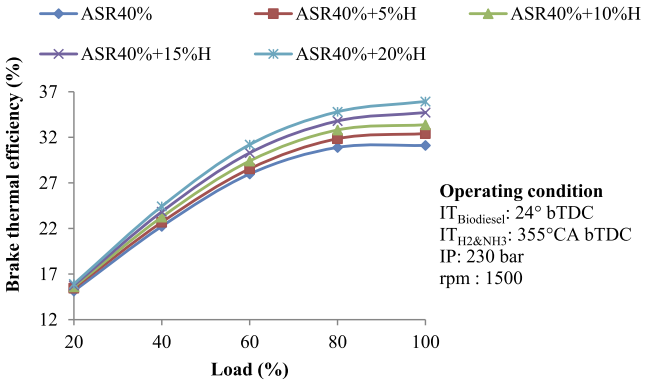

Figure 8. Interaction of BTE with respect to load.

the BTE fluctuations regarding the engine load. As hydrogen is enriched with ammonia, thermal efficiency is enhanced irrespective of load because of its superior properties. At maximum load, the recorded BTE was 31, 32.4, 33.4, 34.7, and 35.9% for ASR40%, ASR40% + 5% H, ASR40% + 10% H, ASR40% + 15% H, and ASR40% + 20% H operations, respectively. In comparison to ASR40% combustion, the observed BTE is improved by 4.2, 7.3, 11.6, and 15.5%. This is because a large amount of gaseous fuel enters the combustion zone and forms a homogeneous mixture, directed injected biodiesel acts as an ignition source, releasing more heat at the premixed burning phase. Because of the rapid flame speed of hydrogen, the flame travels up to the cylinder wall, where the flame developed by the ASR40% combustion might not spread, causing ammonia to escape and the ammonia mixture near the walls of the cylinder to fail to burn, resulting in a misfire.[31] Consequently, the introduction of hydrogen into the optimal ammonia−biodiesel combustion process increases the combustion efficiency and improves the BTE.

3.2.2. Brake Specific Energy Consumption. The BSEC is the amount of energy used to generate unit power. The BSEC is a measure of how effectively an engine utilizes energy and is dependent on fuel properties. BSEC is a suitable indication for assessing the efficiency of an IC engine using different fuels. Figure 9 shows how BSEC levels fluctuate based on hydrogen

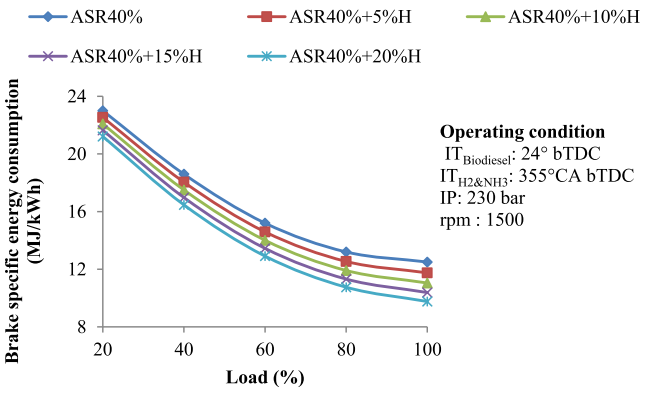

Figure 9. Interaction of brake specific energy consumption with respect to load.

enrichment, depending on engine load. Maximum BSEC was obtained for ASR40% combustion because the heating capacity of the charge mixture was reduced to 23 MJ/kW h. Due to ammonia's lower heating qualities, a greater amount of energy was needed to maintain the identical power, and the combustion rate of the charge mixture was hindered by ammonia's physicochemical characteristics, thus increasing the BSEC.

At maximum load, the measured BSEC was 12.5, 11.75, 11.05, 10.38, and 9.77 MJ/kW h for ASR40%, ASR40% + 5% H, ASR40% + 10% H, ASR40% + 15% H, and ASR40% + 20% H operations, respectively. In comparison to ASR40% combustion, the BSEC decreased by 6.9, 11.6, 16.9, and 21.9%, respectively. Hydrogen addition exhibits reduced BSEC. The low BSEC is due to the appropriate hydrogen mixing with ammonia; hydrogen combusts the ammonia, decreases the exhaust ammonia, and aids in achieving near-complete combustion.[32,33] As the load increases, the BSEC exhibits a decreasing trend. As the load increases, the cylinder wall temperature increases, which leads to an increased fuel oxidation level and improved combustion. Furthermore, when hydrogen is inducted into the combustion, the BSEC starts decreasing. It is likely that the lower volumetric heating capacity of hydrogen might be the cause for the drop in BSEC. As the hydrogen premixing increases, the amount of air required for the charge mixture is reduced because hydrogen has a greater stoichiometric ratio; nevertheless, ammonia has a reduced stoichiometric ratio.

3.3. Emission Factors. *3.3.1. Hydrocarbon Emission.* Hydrocarbons, or more accurately, organic emissions, are triggered by the incomplete combustion of hydrocarbon fuel. Due to high viscosity and poor atomization, HC emissions are associated with the combustion process of biodiesel. The HC emission measured at maximum load was 53, 50, 46, 42, and 40 ppm for ASR40%, ASR40% + 5% H, ASR40% + 10% H, ASR40% + 15% H, and ASR40% + 20% H processes, respectively. In comparison to the ASR40% process, the exhaust HC emission was decreased by 5.6, 13.2, 20.75, and 24.53%.

https://doi.org/10.1021/acsomega.3c06327
ACS Omega XXXX, XXX, XXX−XXX

The hydrogen-enriched ASR40% combustion provided lower HC emissions due to enhanced combustion, as demonstrated in Figure 10. The quantity of HC emissions

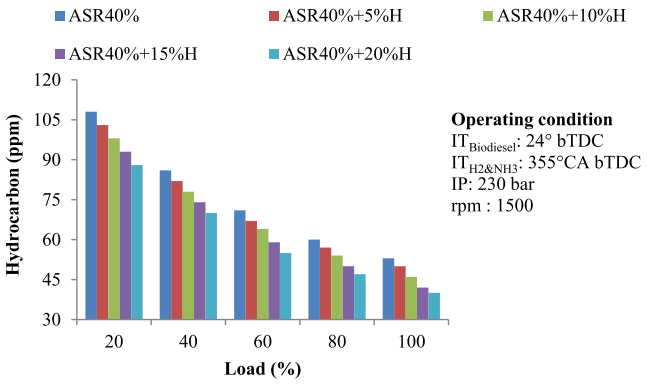

Figure 10. Interaction of hydrocarbon emission with respect to load.

decreases when the load increases because the combustion temperature for the higher load is greater, hence the fuel combustion is improved. In addition, the optimal 40% ammonia−biodiesel operation emits higher HC emissions as ammonia has inferior diffusivity; hence, it creates a biodiesel-rich mixture and forms an inappropriate air fuel ratio, which increases HC emissions. Furthermore, since gaseous ammonia induction reduces oxygen availability in the air, local air-fuel ratios drop. Another possibility is that the ammonia fuel absorbs heat as a consequence of the latent heat of vaporization, lowering cylinder temperatures and decreasing HC oxidation. This tendency is managed by hydrogen enrichment because H_2 has an impressive stoichiometric ratio. As a result of hydrogen's faster flame propagation and greater diffusivity, the inclusion of hydrogen to ASR40% causes the improved air fuel combination to burn fully and rapidly, reducing the quantity of exhaust HC emissions. In addition, hydrogen also has no carbon content in its structure.

3.3.2. Carbon Monoxide Emission. CO is formed during the combustion of fuel-rich mixtures due to a deficiency of oxygen and combustion temperature. The exhaust CO emissions under maximum load conditions were 0.103, 0.095, 0.087, 0.08, and 0.074% volume for ASR40%, ASR40% + 5% H, ASR40% + 10% H, ASR40% + 15% H, and ASR40% + 20% H operations, respectively. In comparison to ASR40% combustion, exhaust CO emissions decreased by 7.8, 15.5, 22.3, and 28.2%. Figure 11 shows the exhaust CO

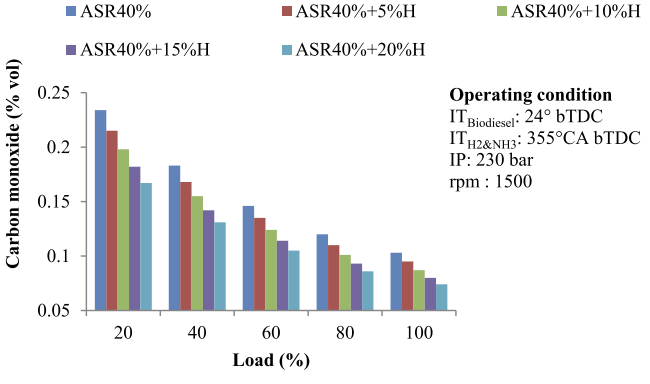

Figure 11. Interaction of CO with respect to load.

emissions with regard to load. The absence of carbon in the hydrogen structure is responsible for the additional drop in the level of CO in the hydrogen-enhanced ammonia−biodiesel process. As the load increases, exhaust CO emissions decrease. This is because the built-in biodiesel oxygen concentration and combustion temperature are significantly higher, which promotes the combustion rate. Hydrogen enrichment could decrease exhaust CO because hydrogen enrichment in the charge decreases the C/H proportion. Also, higher hydrogen diffusivities make the combustible charge more uniform so more oxygen can be used to speed up the burning process. This leads to a faster combustion reaction inside the combustion chamber. Furthermore, OH radicals produced during hydrogen combustion improved the conversion of CO to CO_2, resulting in decreased CO emissions.[34] Optimal 40% ammonia−biodiesel powered RCCI operation results in substantial CO emissions because direct injection biodiesel's higher viscosity causes poor atomization and inappropriate air−fuel mixing, which has the potential to cause flame quenching.

3.3.3. Nitrogen Oxide Emission. The combustion temperature, time, and oxygen concentration all have substantial influences on NOx production. Thermal NOx is produced by the elevated-temperature oxidation of diatomic nitrogen present in combusted air. The rate of production is mostly determined by the temperature and the nitrogen residence time. In accordance with the combustion-science principle, the fundamental source of fuel NOx formation is the fuel nitrogen oxidation process. The exhaust NOx emissions under maximum load conditions were 462, 497, 526, 561, and 609 ppm for ASR40%, ASR40% + 5% H, ASR40% + 10% H, ASR40% + 15% H, and ASR40% + 20% H operations, respectively. The exhaust NOx emissions increased by 7.6, 13.9, 21.4, and 31.8% compared with the ASR40% combustion. Figure 12 shows that NOx emissions from hydrogen

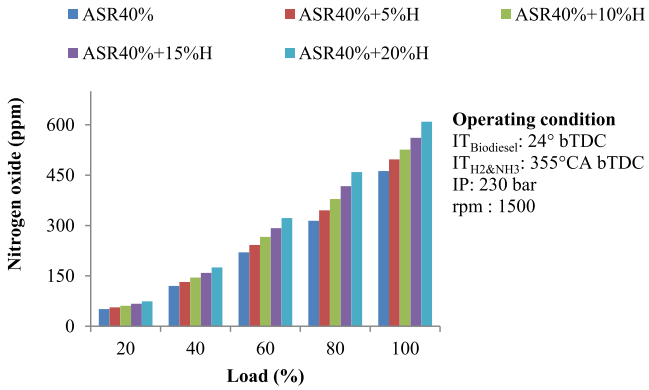

Figure 12. Interaction of NOx with respect to load.

enrichment were greater than those from optimal 40% ammonia−biodiesel combustion under all operating conditions. The fuel NOx formation is explained in eqs 3−14.

3.3.3.1. Formation of Ammonia NOx. The primary ammonia (NH_3) oxidation routes breakdown in the H abstraction processes

$$NH_3 + H \rightarrow NH_2 + H_2 \quad (3)$$

$$NH_3 + OH \rightarrow NH_2 + H_2O \quad (4)$$

$NH_2 \rightarrow$ NH of H abstraction oxidation reactions[35]

https://doi.org/10.1021/acsomega.3c06327
ACS Omega XXXX, XXX, XXX−XXX

$$NH_2+OH \rightarrow NH+H_2O \quad (5)$$

$$NH_2+H \rightarrow NH+H_2 \quad (6)$$

The most important processes responsible for the creation of intermediary HNO molecules are

$$NH_2+O \rightarrow HNO + H \quad (7)$$

(most prevalent reaction in NO production).

Equation 7 has a branching reaction:

NO formation reactions

$$NH + OH \rightarrow HNO + H \quad (8)$$

$$NH+O_2 \rightarrow HNO + O \quad (9)$$

$$NH + O \rightarrow NO + H \quad (10)$$

$$NH+O_2 \rightarrow NO + OH \quad (11)$$

For intermediate species of HNO, eqs 8 and 9 involve interactions of NH with active radicals. The interactions of NH with active radicals in eqs 10 and 11 are used for immediate NO decomposition.[36]

The final outcomes of the HNO → NO breakdown process are as follows

$$HNO + H \rightarrow NO+H_2 \quad (12)$$

$$HNO \rightarrow NO + H \quad (13)$$

$$HNO + OH \rightarrow NO+H_2O \quad (14)$$

Furthermore, hydrogen addition in the ASR40% mixture increased exhaust NOx due to the increased premixed combustion, and there was a rise in flame temperature, which is associated with high NOx emissions. Another explanation might be that due to the higher heating capacity of hydrogen fuel, a larger quantity of heat is released, causing this tendency. The NOx emissions were considerably reduced when the ASR40% combustion operation was used. This was caused by the addition of NH_3, which caused thermal stratification and absorbed thermal energy, decreasing the local in-cylinder combustion temperature where NOx actively develops.[37]

3.3.4. Smoke Opacity. Improper air−fuel mixtures and an inadequate quantity of oxygen in combustion result in inefficient fuel combustion, which leads to smoke formation. The exhaust smoke opacity was measured under maximum load conditions to be 39.5, 37.1, 34.3, 31.7, and 29.3% for ASR40%, ASR40% + 5% H, ASR40% + 10% H, ASR40% + 15% H, and ASR40% + 20% H hydrogen-enrichment operations, respectively. The observed exhaust smoke opacity was reduced by 6.1, 13.2, 19.8, and 25.8% compared to ASR40% combustion. Figure 13 shows that the optimal 40% ammonia−biodiesel combustion with 20% hydrogen enrichment reduces smoke more significantly under all engine load conditions. Because of more substantial hydrogen mass diffusivity, which mixes with oxygen quicker and combusted more easily in the premixed combustion. Biodiesel has a positive influence on smoke opacity since it does not totally vaporize. Furthermore, when load increases, the smoke observed for the test fuel increases dramatically because fuel consumption increases, causing smoke opacity to increase as well. Similar results have been reported in the literature.[38] Another possible reason is that when combustion is initiated because of its rapid flame speed, premixed hydrogen begins to burn prior to the injected biodiesel being mixed with oxygen.

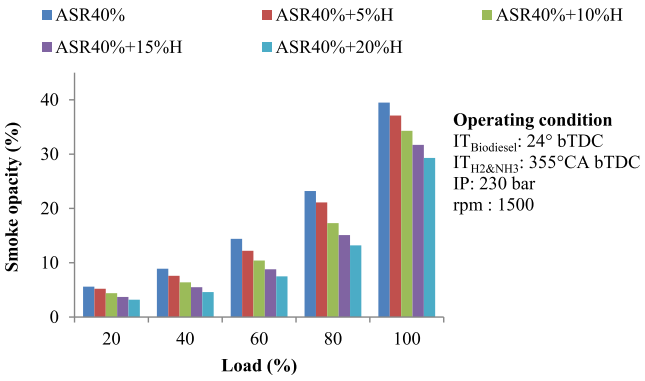

Figure 13. Interaction of smoke opacity with respect to load.

Next, for higher loads, the fuel/air equivalency ratio results in a higher smoke concentration. When the concentration of hydrogen increases, less smoke forms than in any other region. This impact is mostly due to the longer premixed controlled combustion. However, the smoke is worse in the area with higher loads. The lower oxygen content is the cause of the greater fuel consumption and reduction in volumetric efficiency due to premixed ammonia and hydrogen. Additionally, there is a short period of time to combust the greatly increased fuel supply.

3.3.5. Exhaust Gas Temperature. The temperature of the exhaust gas reveals how well a fuel's heat energy is being used. Heat loss in the exhaust pipe or a rise in exhaust temperature lowers the fuel's conversion of heat energy to work. The exhaust gas temperature (EGT) was measured under maximum load conditions to be 458, 434, 419, 396, and 378 °C for ASR40%, ASR40% + 5% H, ASR40% + 10% H, ASR40% + 15% H, and ASR40% + 20% H operations, respectively. In comparison to ASR40% combustion, the EGT was lowered by 5.23, 8.5, 13.5, and 17.5%, respectively. Slow-burning fuel causes a prolonged afterburn duration, which increases the EGT. Figure 14 depicts the impact of EGT on

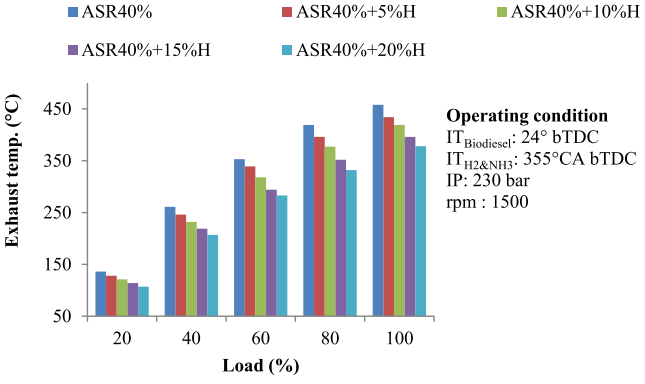

Figure 14. Interaction of EGT with respect to load.

the load for the test fuels. When hydrogen is introduced to the optimal 40% ammonia−biodiesel operation, the combustion efficiency advances and the EGT lowers.[39] EGT rises when the load rises because more heat is generated by burning more fuel. The ASR40% combustion, on the other hand, has a greater engine exhaust temperature. This might be due to the long after-burning duration, which allows some quantity to burn at the late combustion stage, increasing the exhaust temperature.[40,41] As the hydrogen concentration in the combustion

https://doi.org/10.1021/acsomega.3c06327
ACS Omega XXXX, XXX, XXX−XXX

increased, premixing combustion increased and the late combustion phase decreased, therefore increasing combustion temperature, where NOx actively forms, and at the same time, conversion efficiency increased. As a result, NOx and BTE increased, and EGT decreased.

4. CONCLUSIONS

The present study is an attempt to substantiate the potential use of ammonia as a fuel when it is utilized with hydrogen enrichment in 40% ammonia−biodiesel of the dual-fuel RCCI engine by investigating combustion, performance, and emission characteristics. Based on the experimental analysis, the following conclusions are observed:

- The 20% hydrogen-enriched 40% ammonia−biodiesel combustion improved the CP, peak HRR, and CHRR by 15.12, 25.15, and 26.68%, respectively. ID and CD were reduced by 15.53 and 11.24%, respectively. The combustion phasing angle was advanced to 4 °CA at maximum load conditions.
- BTE was increased by 15.49%, and BSEC was reduced by 21.92%, while the NO level was significantly increased by about 31.82%, and HC, CO, smoke, and EGT were reduced by 24.53, 28.16, 25.82, and 17.47% at maximum load conditions.

4.1. Admonition of the Investigation with an Understanding of the Obtained Results. This research is important for understanding how carbon-free energy will affect future industrial and transportation systems. The importance of carbon-free energy in the transportation industry is rising as a result of growing environmental concerns and the need for sustainable energy sources. The findings of this research provide insightful information about the possibilities for carbon-free energy in this sector and emphasize the significance of creating innovative solutions to enhance the performance and emissions of engines that use ammonia as fuel. The hydrogen enrichment of the biodiesel-ignited ammonia fuel has shown significant enhancements in performance, exhaust emissions, and energy parameters at substantially all engine load conditions. Therefore, this approach may be used to lessen the dependence on traditional diesel fuel in both the on-road and off-road transportation sectors.

AUTHOR INFORMATION

Corresponding Author

Ravi Krishnaiah − *School of Mechanical Engineering, VIT University, Vellore 632014, India;* orcid.org/0000-0001-7911-0437; Email: ravi.krishnaiah@vit.ac.in

Authors

Elumalai Ramachandran − *School of Mechanical Engineering, VIT University, Vellore 632014, India;* orcid.org/0000-0002-4970-8777

Elumalai Perumal Venkatesan − *Department of Mechanical Engineering, Aditya Engineering College, Surampalem 533437, India;* orcid.org/0000-0002-7536-8200

Sreenivasa Reddy Medapati − *Department of Mechanical Engineering, Aditya Engineering College, Surampalem 533437, India*

Rajagopalan Sabarish − *Department of Mechanical Engineering, Bharath Institute of Higher Education and Research, Chennai 600 073, India*

Sher Afghan Khan − *Department of Mechanical Engineering, IIUM, Kuala Lumpur 53100, Malaysia*

Mohammad Asif − *Department of Chemical Engineering, King Saud University, Riyadh 11421, Saudi Arabia*

Emanoil Linul − *Department of Mechanics and Strength of Materials, Politehnica University Timisoara, 300222 Timisoara, Romania*

Complete contact information is available at: https://pubs.acs.org/10.1021/acsomega.3c06327

Notes

The authors declare no competing financial interest.

ACKNOWLEDGMENTS

The financial support from the Researchers Supporting Project (RSP2023R42), King Saud University, Riyadh, Saudi Arabia is appreciated. The authors thank the School of Mechanical Engineering, Vellore Institute of Technology, Vellore, for the financial support for this work.

REFERENCES

(1) Kukana, R.; Jakhar, O. P. Performance, combustion and emission characteristics of a diesel engine using composite biodiesel from waste cooking oil - Hibiscus Cannabinus oil. *J. Cleaner Prod.* **2022**, *372*, 133503.

(2) Shrivastava, P.; Rajak, U.; Nashine, P.; Verma, T. N. Performance and Emission Characteristics of a Compression Ignition Engine Fueled With Roselle and Karanja Biodiesel. *Roselle Production, Processing, Products and Biocomposites*; Elsevier Science, 2021; pp 165−176..

(3) Tizvir, A.; Shojaeefard, M. H.; Zahedi, A.; Molaeimanesh, G. R. Performance and emission characteristics of biodiesel fuel from Dunaliella tertiolecta microalgae. *Renewable Energy* **2022**, *182*, 552−561.

(4) Ogunkunle, O.; Ahmed, N. A. Exhaust emissions and engine performance analysis of a marine diesel engine fulled with Parinari polyandra biodiesel-diesel blends. *Energy Rep.* **2020**, *6*, 2999−3007.

(5) Raman, L. A.; Deepanraj, B.; Rajakumar, S.; Sivasubramanian, V. Experimental investigation on performance, combustion and emission analysis of a direct injection diesel engine fuelled with rapeseed oil biodiesel. *Fuel* **2019**, *246*, 69−74.

(6) Olabi, A. G.; Abdelkareem, M. A.; Al-Murisi, M.; Shehata, N.; Alami, A. H.; Radwan, A.; Wilberforce, T.; Chae, K. J.; Sayed, E. T. Recent progress in Green Ammonia: Production, applications, assessment; barriers, and its role in achieving the sustainable development goals. *Energy Convers. Manage.* **2023**, *277*, 116594.

(7) Mi, S.; Wu, H.; Pei, X.; Liu, C.; Zheng, L.; Zhao, W.; Qian, Y.; Lu, X. Potential of ammonia energy fraction and diesel pilot-injection strategy on improving combustion and emission performance in an ammonia-diesel dual fuel engine. *Fuel* **2023**, *343*, 127889.

(8) Subramani, A. K.; Duraisamy, G.; Govindan, N.; Hossain, A. K. An innovative method of ammonia use in a light-duty automotive diesel engine to enhance diesel combustion, performance, and emissions. *Int. J. Hydrogen Energy* **2023**.

(9) Wu, X.; Feng, Y.; Gao, Y.; Xia, C.; Zhu, Y.; Shreka, M.; Ming, P. Numerical simulation of lean premixed combustion characteristics and emissions of natural gas-ammonia dual-fuel marine engine with the pre-chamber ignition system. *Fuel* **2023**, *343*, 127990.

(10) Dinesh, M. H.; Kumar, G. N. Experimental investigation of variable compression ratio and ignition timing effects on performance, combustion, and Nox emission of an ammonia/hydrogen-fuelled Si engine. *Int. J. Hydrogen Energy* **2023**.

(11) Köse, H.; Ciniviz, M. An experimental investigation of effect on diesel engine performance and exhaust emissions of addition at dual fuel mode of hydrogen. *Fuel Process. Technol.* **2013**, *114*, 26−34.

https://doi.org/10.1021/acsomega.3c06327
ACS Omega XXXX, XXX, XXX−XXX

(12) Qin, Z.; Yang, Z.; Jia, C.; Duan, J.; Wang, L. Experimental study on combustion characteristics of diesel-hydrogen dual-fuel engine. *J. Therm. Anal. Calorim.* **2020**, *142* (4), 1483−1491.
(13) Gültekin, N.; Gülcan, H. E.; Ciniviz, M. Investigation of the effects of hydrogen energy ratio and valve lift amount on performance and emissions in a hydrogen-diesel dual-fuel compression ignition engine. *Int. J. Hydrogen Energy* **2023**.
(14) Anchupogu, P.; Krupakaran, R. L.; Venkateswarlu, S.; Satish, S.; Phaneendrareddy, S.; Shohel, S.; Umamaheswarrao, P. Combined effect of hydrogen and with Julifora biodiesel blend (JFB20) on the combustion, performance and emission characteristics of a direct-injection diesel engine. *Mater. Today: Proc.* **2023**.
(15) Purayil, S. T. P.; Al-Omari, S.; Elnajjar, E. Effect of Hydrogen Blending on the Combustion Performance, Emission, and Cycle-to-Cycle Variation Characteristics of a Single-Cylinder GDI Spark Ignition Dual-Fuel Engine. *Int. J. Thermofluids* **2023**, *20*, 100403.
(16) Curran, S. J.; Hanson, R. M.; Wagner, R. M. Reactivity controlled compression ignition combustion on a multi-cylinder light-duty diesel engine. *Int. J. Engine Res.* **2012**, *13* (3), 216−225.
(17) Tamilvanan, A.; Mohanraj, T.; Ashok, B.; Santhoshkumar, A. Enhancement of energy conversion and emission reduction of Calophyllum inophyllum biodiesel in diesel engine using reactivity controlled compression ignition strategy and TOPSIS optimization. *Energy* **2023**, *264*, 126168.
(18) Liu, J.; Ma, H.; Wang, L.; Liang, W.; Ji, Q.; Sun, P.; Wang, P. Effects of EGR on combustion and emission characteristics of PODE/methanol RCCI mode at high load. *Appl. Therm. Eng.* **2023**, *223*, 120036.
(19) Nadimi, E.; Przybyła, G.; Lewandowski, M. T.; Adamczyk, W. Effects of ammonia on combustion, emissions, and performance of the ammonia/diesel dual-fuel compression ignition engine. *J. Energy Inst.* **2023**, *107*, 101158.
(20) Kobayashi, H.; Hayakawa, A.; Somarathne, K. D. K. A.; Okafor, E. C. Science and technology of ammonia combustion. *Proc. Combust. Inst.* **2019**, *37* (1), 109−133.
(21) Pinto, G. M.; de Souza, T.; da Costa, R.; Roque, L.; Frez, G.; Coronado, C. Combustion, performance and emission analyses of a CI engine operating with renewable diesel fuels (HVO/FARNESANE) under dual-fuel mode through hydrogen port injection. *Int. J. Hydrogen Energy* **2023**, *48*, 19713−19732.
(22) Xin, G.; Ji, C.; Wang, S.; Meng, H.; Chang, K.; Yang, J. Effect of ammonia addition on combustion and emission characteristics of hydrogen-fueled engine under lean-burn condition. *Int. J. Hydrogen Energy* **2022**, *47* (16), 9762−9774.
(23) Kumar, C. B.; Lata, D. B.; Mahto, D. Analysis of ignition delay by taking Di-tertiary-butyl peroxide as an additive in a dual fuel diesel engine using hydrogen as a secondary fuel. *Int. J. Hydrogen Energy* **2020**, *45* (29), 14806−14820.
(24) Parthasarathy, M.; Ramkumar, S.; Elumalai, P. V.; Kumar Gupta, S.; Krishnamoorthy, R.; Mohammed Iqbal, S.; Kumar Dash, S.; Silambarasan, R. Experimental investigation of strategies to enhance the homogeneous charge compression ignition engine characteristics powered by waste plastic oil. *Energy Convers. Manage.* **2021**, *236*, 114026.
(25) Xin, G.; Ji, C.; Wang, S.; Meng, H.; Chang, K.; Yang, J. Effect of different volume fractions of ammonia on the combustion and emission characteristics of the hydrogen-fueled engine. *Int. J. Hydrogen Energy* **2022**, *47* (36), 16297−16308.
(26) Shrestha, K. P.; Lhuillier, C.; Barbosa, A. A.; Brequigny, P.; Contino, F.; Mounaïm-Rousselle, C.; Seidel, L.; Mauss, F. An experimental and modeling study of ammonia with enriched oxygen content and ammonia/hydrogen laminar flame speed at elevated pressure and temperature. *Proc. Combust. Inst.* **2021**, *38* (2), 2163−2174.
(27) Gültekin, N.; Ciniviz, M. Examination of the effect of combustion chamber geometry and mixing ratio on engine performance and emissions in a hydrogen-diesel dual-fuel compression-ignition engine. *Int. J. Hydrogen Energy* **2023**, *48* (7), 2801−2820.
(28) Wang, B.; Yang, C.; Wang, H.; Hu, D.; Wang, Y. Effect of Diesel-Ignited Ammonia/Hydrogen Mixture Fuel Combustion on Engine Combustion and Emission Performance. *SSRN Electron. J.* **2023**, *331*, 125865.
(29) Chen, Z.; Wang, L.; Zeng, K. Comparative study of combustion process and cycle-by-cycle variations of spark-ignition engine fueled with pure methanol, ethanol, and n-butanol at various air-fuel ratios. *Fuel* **2019**, *254*, 115683.
(30) Caton, J. A. Combustion phasing for maximum efficiency for conventional and high efficiency engines. *Energy Convers. Manage.* **2014**, *77*, 564−576.
(31) Kiran, S.; Martin, M. L. J.; Sonthalia, A.; Varuvel, E. G. Synergistic effect of hydrogen and waste lubricating oil on the performance and emissions of a compression ignition engine. *Int. J. Hydrogen Energy* **2023**, *48*, 23296−23307.
(32) Wang, B.; Yang, C.; Wang, H.; Hu, D.; Wang, Y. Effect of Diesel-Ignited Ammonia/Hydrogen mixture fuel combustion on engine combustion and emission performance. *Fuel* **2023**, *331*, 125865.
(33) Juknelevičius, R.; Rimkus, A.; Pukalskas, S.; Matijošius, J. Research of performance and emission indicators of the compression-ignition engine powered by hydrogen - Diesel mixtures. *Int. J. Hydrogen Energy* **2019**, *44* (20), 10129−10138.
(34) Wang, Y.; Zhou, X.; Liu, L. Theoretical investigation of the combustion performance of ammonia/hydrogen mixtures on a marine diesel engine. *Int. J. Hydrogen Energy* **2021**, *46* (27), 14805−14812.
(35) Sumathi, R.; Sengupta, D.; Nguyen, M. T. Theoretical study of the H2 + NO and related reactions of [H2NO] isomers. *J. Phys. Chem. A* **1998**, *102* (18), 3175−3183.
(36) Elbaz, A. M.; Wang, S.; Guiberti, T. F.; Roberts, W. L. Review on the recent advances on ammonia combustion from the fundamentals to the applications. *Fuel Commun.* **2022**, *10*, 100053.
(37) Liu, L.; Wu, J.; Liu, H.; Wu, Y.; Wang, Y. Study on marine engine combustion and emissions characteristics under multi-parameter coupling of ammonia-diesel stratified injection mode. *Int. J. Hydrogen Energy* **2023**, *48*, 9881−9894.
(38) Singh Kalsi, S.; Subramanian, K. A. Experimental investigations of effects of EGR on performance and emissions characteristics of CNG fueled reactivity controlled compression ignition (RCCI) engine. *Energy Convers. Manage.* **2016**, *130*, 91−105.
(39) Kurien, C.; Mittal, M. Review on the production and utilization of green ammonia as an alternate fuel in dual-fuel compression ignition engines. *Energy Convers. Manage.* **2022**, *251*, 114990.
(40) Murugesan, P.; Elumalai, P.; Balasubramanian, D.; Padmanabhan, S.; Murugunachippan, N.; Afzal, A.; Sharma, P.; Kiran, K.; Femilda Josephin, J.; Varuvel, E. G.; et al. Exploration of low heat rejection engine characteristics powered with carbon nanotubes-added waste plastic pyrolysis oil. *Process Saf. Environ. Prot.* **2023**, *176*, 1101−1119.
(41) Hoang, A. T.; Murugesan, P.; Pv, E.; Balasubramanian, D.; Parida, S.; Priya Jayabal, C.; Nachippan, M.; Kalam, M.; Truong, T. H.; Cao, D. N.; et al. Strategic combination of waste plastic/tire pyrolysis oil with biodiesel for natural gas-enriched HCCI engine: Experimental analysis and machine learning model. *Energy* **2023**, *280*, 128233.

https://doi.org/10.1021/acsomega.3c06327
ACS Omega XXXX, XXX, XXX−XXX